Rubbing-Induced Vibration Response Analysis of Dual-Rotor-Casing System

Ma Xinxing[1], *Ma Hui*[1,2*], *Zeng Jin*[1], *Piao Yuhua*[1]

1. School of Mechanical Engineering and Automation, Northeastern University, Shenyang 110819, P. R. China; 2. State Key Laboratory of Mechanical System and Vibration, Shanghai Jiao Tong University, Shanghai 200240, P. R. China

(Received 4 November 2017; revised 17 January 2018; accepted 20 January 2018)

Abstract: Considering gyroscopic effects caused by rotational speed, torsional vibration as well as coupling effects among inner rotor, out rotor and casing, a dynamic model of the dual-rotor-casing system is established using finite element (FE) method. By comparing the natural characteristics obtained from MATLAB and ANSYS, the developed model is verified. Then rubbing-induced vibration responses in dual-rotor-casing system are analyzed. The effects of rotational speed and speed ratio on rubbing vibration responses of the system are discussed. Results show that different combined frequency components will appear in the spectrum except two unbalanced excitation frequencies and their multiple frequency components, and these frequencies can be used as the dual-rotor aero-engine rubbing failure diagnosis frequencies when rubbing occurs. Besides, the amplitude of torsional vibration is larger than that of lateral vibration under the same working condition, and speed ratio has a great impact on the periodicity of the system rubbing-induced motion trajectory. The amplitude of rubbing-induced responses under counter-rotation is less than that under co-rotation with the same parameters.

Key words: dual-rotor-casing system; rubbing fault; finite element method; coupling dynamic

CLC number: V231.9 **Document code**: A **Article ID**: 1005-1120(2018)01-0101-08

0 Introduction

According to the difference of contact area, the rubbing can be divided into the following four categories: Fixed point rubbing, partial rubbing, full annual rubbing and partial rubbing mixed with fixed point rubbing[1]. Researches on rubbing rotor system have been studied by many scholars[2-7]. Based on a dynamic model of rotor-stator rubbing proposed by Muszynska[1], Yan et al.[8] developed a simplified model of rotor-stator rub-impact for a kind of dual-rotor engine. The vibration characteristics for some types of rubbing for the dual-shaft engine are analyzed, the theoretical results are consistent with data measured on a dual-shaft aircraft engine. Yang et al.[9-10] established a kinetic model of aero engine considering imbalances and fixed point rubbing, furthermore, a new model of rubbing force with coating painted on the discs and casing is established based on the Lankarani-Nikravesh model. Xu et al.[11] simplified the stator in a dual-rotor system into a flexible sheet from a new perspective, taking into account the effect of the elastic deformation of the sheet and the amount of intrusion caused by the contact. Collision force and friction were calculated by utilizing Hertz contact theory and Coulomb model. The transient dynamic response of the whole aero-engine under the rubbing fault is analyzed. Zhou et al.[12] established the coupling dynamic model of the dual rotor-ball bearing-stator, considering the rolling bearing gap and the nonlinear Hertz contact force. The vibration responses of the system were obtained from numerical integral method, and the

* Corresponding author, E-mail address: mahui_2007@163.com.

How to cite this article: Ma Xinxing, Ma Hui, Zeng Jin, et al. Rubbing-induced vibration response analysis of dual-rotor-casing system[J]. Trans. Nanjing Univ. Aero. Astro., 2018,35(1):101-108.
http://dx.doi.org/10.16356/j.1005-1120.2018.01.101

phenomenon of beat vibration of the dual rotor system is analyzed. Finally, the influence of different speed ratios and rubbing stiffness on the dynamic characteristics of the system is discussed.

Most of the scholars mentioned earlier use numerical simulation to analyze the dual-rotor system rubbing response[13-15], and some scholars simulate the rubbing response by commercial software. Han et al.[16] established the local rubbing model of the dual-rotor system using MSC. ADAMS software based on the rigid-flexible multi-body model, and analyzed the nonlinear dynamic characteristics of the system. Aiming at the shortcomings of the traditional model of the impact force model, Wang et al.[17] established the finite element (FE) model of the rotor shaft and obtained the first six-order natural frequencies of the rotor system by ANSYS. By the methods of spectrum and cepstrum analysis, the rubbing characteristics of the casing vibration acceleration time series data are analyzed. The results show that the casing vibration acceleration has obvious impact characteristics.

From the literatures listed above, conclusions can be made that most researches concentrate on the dynamic characteristics of a dual-rotor system without casing. Nevertheless, the presence of the casing will have a great impact on the vibration response of the system. In terms of structural integrity, the dual-rotor-casing coupling system is closer to the aero-engine. In addition, the vibration responses (displacement/acceleration) of the stator such as casing have been paid more attention because of the convenience of signal collection. In this paper, the casing is modeled using Timoshenko beam element and rubbing-induced vibration responses in dual-rotor-casing system are analyzed.

1 Dynamic Model of Dual-Rotor-Casing System

1.1 FE model of dual-rotor-casing system

In this paper, the rubbing in dual-rotor-casing system is analyzed. Schematic of the model is shown in Fig. 1. The low-pressure (LP) rotor and high-pressure (HP) rotor subsystems include one rigid compressor disc and one rigid turbine disc. The bearing is simulated by the linear spring and damping elements. LP and HP rotors are connected by inter-shaft bearing, the coupling of two-rotor subsystems could be considered. By FE discretization, the rotors are divided into 19 elements and 21 nodes while the casing is discretized into 15 elements. The inner rotor, outer rotor and the casing are modeled by Timoshenko beam element. In order to consider the torsional vibration, each node of LP/HP rotors has five degrees of freedom (DOFs) including two lateral DOFs (u_x, u_y) and three rotational DOFs (rot$x$, rot$y$, rot$z$), while each node of the casing has two lateral DOFs (u_x, u_y) and two rotational DOFs (rot$x$, rot$y$). All the disks are simulated by lumped mass elements.

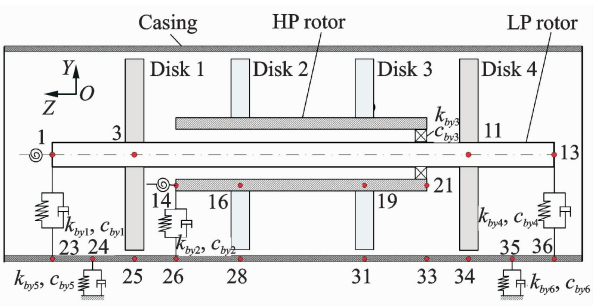

Fig. 1 Schematic of dual-rotor-casing system

In Fig. 1, k_{by1}, k_{by4} and c_{by1}, c_{by4} are the supporting stiffness and damping of the Y direction between the LP rotor and the casing, respectively. k_{by2} and c_{by2} are the supporting stiffness and damping of the Y direction between the HP rotor and the casing. k_{by3} and c_{by3} are the supporting stiffness and damping of the Y direction of inter-bearing. k_{by5}, k_{by6} and c_{by5}, c_{by6} are the supporting stiffness and damping of the Y direction between the casing and the base, respectively.

1.2 Rubbing force model

In order to constrain the rigid casing, the linear spring and damping elements are connected to

the casing, the local-contact elastic deformation caused by contact force is ignored. Fig. 2 illustrates the principle of rubbing between disk and casing. When the system remains stationary, O_d and O_c is the geometric center of LP rotor and casing, respectively. In addition, the casing center O_c coincides with the coordinate system origin O. R_d and R_c denote the radius of rubbing disk and the casing, respectively. e is eccentricity. k_{cx}, k_{cy} and c_{cx}, c_{cy} are the supporting stiffness and damping of the x and y directions between the casing and the base, respectively.

The minimum gap c between the disk and casing, and the eccentricity e can be written as

$$c=R_c-R_d-\sqrt{x_m^2+y_m^2},\ e=\sqrt{x_m^2+y_m^2} \quad (1)$$

where x_m and y_m are the components of the eccentriccity e in the x and y directions.

In actual working conditions, O_d' and O_c', the center of rotor and casing, will deviate from the original position in plane because of the installation error and rubbing. And the radial relative displacement ξ between rotor and casing meets

$$\xi=\sqrt{(x_d-x_c+x_m)^2+(y_d-y_c+y_m)^2} \quad (2)$$

Penetration depth δ between the disk and casing is obtained from

$$\delta=\begin{cases}\xi-e-c & \xi\geqslant e+c\\ 0 & \xi<e+c\end{cases} \quad (3)$$

The rubbing force can be written as

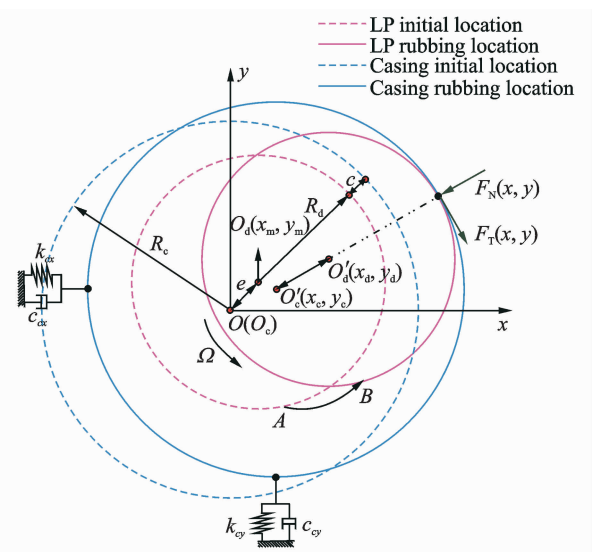

Fig. 2 Schematic diagram of rubbing between disk-casing

$$\begin{cases}F_N(x,y)=k_r\delta\\ F_T(x,y)=\mu F_N\end{cases} \quad \xi\geqslant e+c \quad (4)$$

where F_N is the normal rubbing force, F_T the tangential rubbing force, k_r the contact stiffness, and μ the friction coefficient.

1.3 Model validation

The natural frequencies obtained from ANSYS and MATLAB are listed in Table 1. Comparing the first six natural frequencies, the errors are less than 3%. It demonstrates the validity of the model developed by FE method. Research on the dynamic characteristics in both co-rotation and counter-rotation was conducted. As shown in Fig. 3, Campbell diagrams of these two cases were obtained by calculation of natural frequencies. The forward whirl frequency increases with spin speed while the backward whirl frequencies decreases. One common phenomenon that can be found in two Campbell diagrams is that the torsional frequencies do not change with the increase of spin speed.

Table 1 Natural frequencies comparison of dual rotor (Ω= 0 rev/min)

Order	Natural frequency/Hz		Error/%
	ANSYS	MATLAB	
1	24.273	24.277	0.016
2	35.102	35.002	−0.285
3	35.102	35.002	−0.285
4	74.697	74.714	0.023
5	94.265	94.122	−0.152
6	94.265	94.122	−0.152

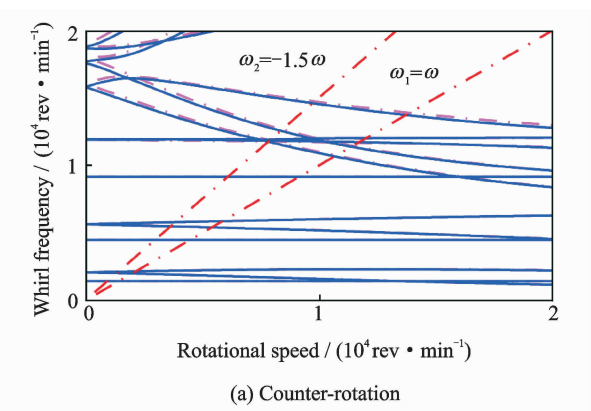

(a) Counter-rotation

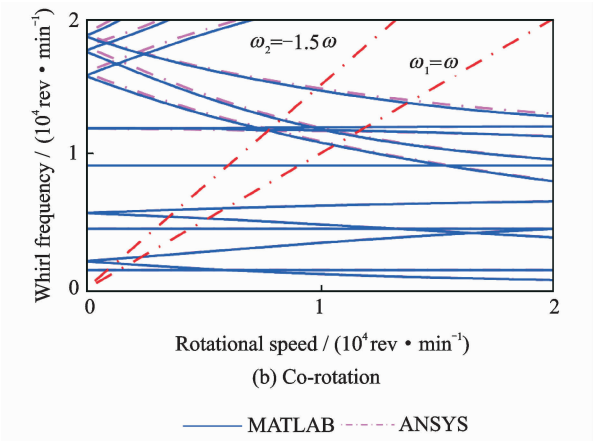

Fig. 3 Campbell diagram of dual-rotor system

2 Rubbing-Induced Vibration Responses in Dual-Rotor-Casing System

In this section, the effects of rotational speed and speed ratio on rubbing-induced vibration responses of the dual-rotor-casing system are discussed in detail. Time-domain waveform, spectrum cascades, and frequency spectrum are used to analyze the vibration responses. It is worth noting that only local rubbing between disk 1 and casing (see Fig. 1) is concerned in this paper.

2.1 Effects of rotational speed

Rotational speed has a significant influence on the vibration responses of the dual-rotor-casing system. The spectrum cascades under the case of different rotational speeds (800—5 800 rev/min) are shown in the rubbing process (see Fig. 4). From Fig. 4, the phenomenon can be distinguished by the separation of the rotational speed of LP rotor. Firstly, when the range of rotational speed is low (800—2 000 rev/min), the rubbing is minor and occurs infrequently. It is easy to found the peak values of f_1 and f_2 are prominent. Secondly, when Ω=1 700 rev/min, rubbing appears frequently and the amplitudes of combined frequency components become obvious. In addition, the spectral line of HP rotor generates resonance (point A) firstly and amplitude amplifies because of the excitation of 1st order natural frequency. After the first critical speed, spectrum cascades are filled with abundant frequency components such as f_2-f_1, $1/2f_2$, $2f_1-f_2$, $2f_1$, f_1+f_2, $2f_2$. The response values of combined frequency components become larger with the increasing rotational speed (2 000—4 000 rev/min). When rotational speed is 2 300 rev/min, the spectral line of LP rotor generates resonance (point B) and amplitude amplification occurs due to the excitation of 1st order natural frequency. At the interval of [4 000, 5 800] rev/min, rubbing becomes very strong, more combined frequencies occur and the 2nd order natural frequency is excited (points C and D).

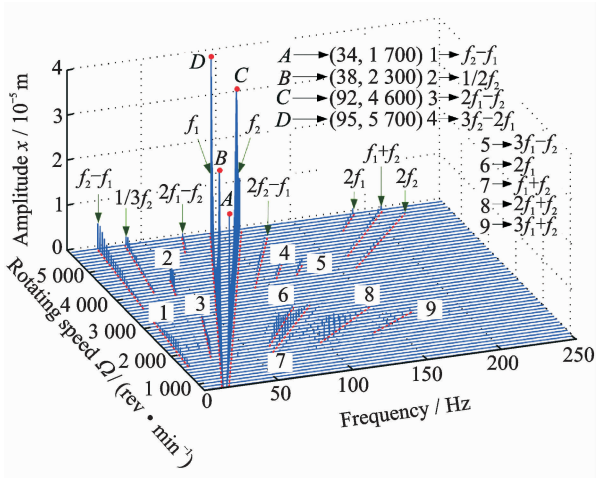

Fig. 4 Spectrum cascades of inner rotor rubbing under different rotational speeds

Vibration responses of LP rotor and casing at Ω= 2 300 rev/min are shown in Fig. 5, the red broken lines in time domain waveform correspond to the time when the rubbing begins. The orbits of the inner rotor and casing are asymmetric and both compressed seriously. In the spectrum, the response frequencies contain more components and amplitude of combined frequencies are dominant. Meanwhile, time domain waveform of torsional displacement at the compressor disc of LP rotor and HP rotor are shown in Fig. 6, respectively. The amplitude of torsional displacement is larger than lateral displacement under the same condition. In order to compare the effect of the casing on the rubbing induced vibration responses, the vibration responses which the casing is simulated as lumped mass are obtained under the same case (see Fig. 7).

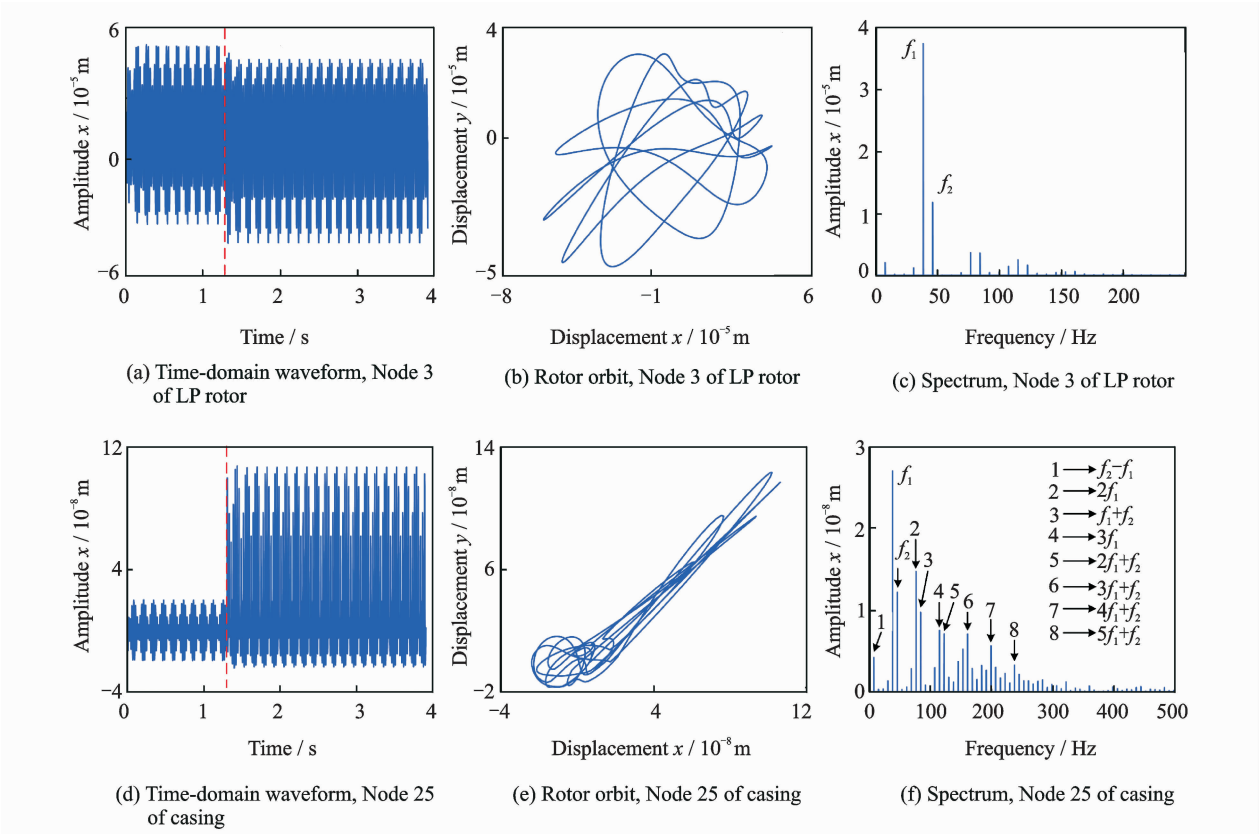

Fig. 5 Rubbing-induced responses at Ω=2 300 rev/min

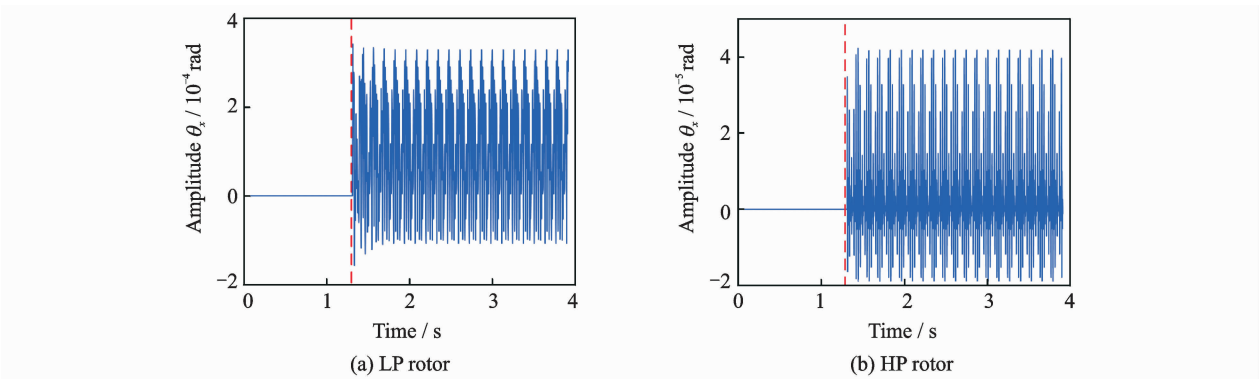

Fig. 6 Torsional displacement at Ω=2 300 rev/min

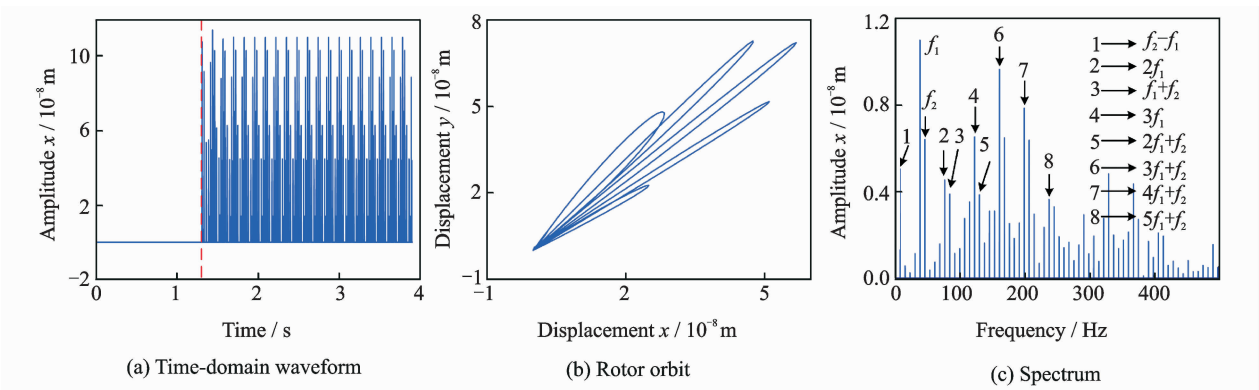

Fig. 7 Rubbing-induced responses of mass point casing at Ω=2 300 rev/min

In Fig. 7, the elastic supports between the dual-rotor and the casing are ignored. It can be seen that the vibration amplitude in Fig. 5 is larger than that in Fig. 7, which indicates that the coupling between rotor and casing has significant effects on the dynamics of the system and should be considered.

2.2 Effects of speed ratio

The dual-rotor system has two operation modes including co-rotation and counter-rotation. Fig. 8 indicates the LP rotor motion trajectory with rubbing under different speed ratios. From the Fig. 8, it can be seen that the motion trajectory under counter-rotation shows petal-like and the number of petals implies the period of motion. When the speed ratio is positive, the motion trajectories are multiple circles. It's worth noting that the response amplitudes under counter-rotation are less than that under co-rotation because the gyro-moment is offset partially. What's more, when 10η is odd number the motion trajectories have more cycles than that when 10η is even.

Fig. 9 shows the rubbing response under $\eta=-1.7$. From the time-domain waveform, it can be found that the change of waveform is not obvious both in LP rotor and casing. In the figure of rotor orbit, petals are crossed. Two rotational-frequencies of dual rotor are prominent and there are also many combined frequency components. Corresponding simulation parameters are listed in Table 2.

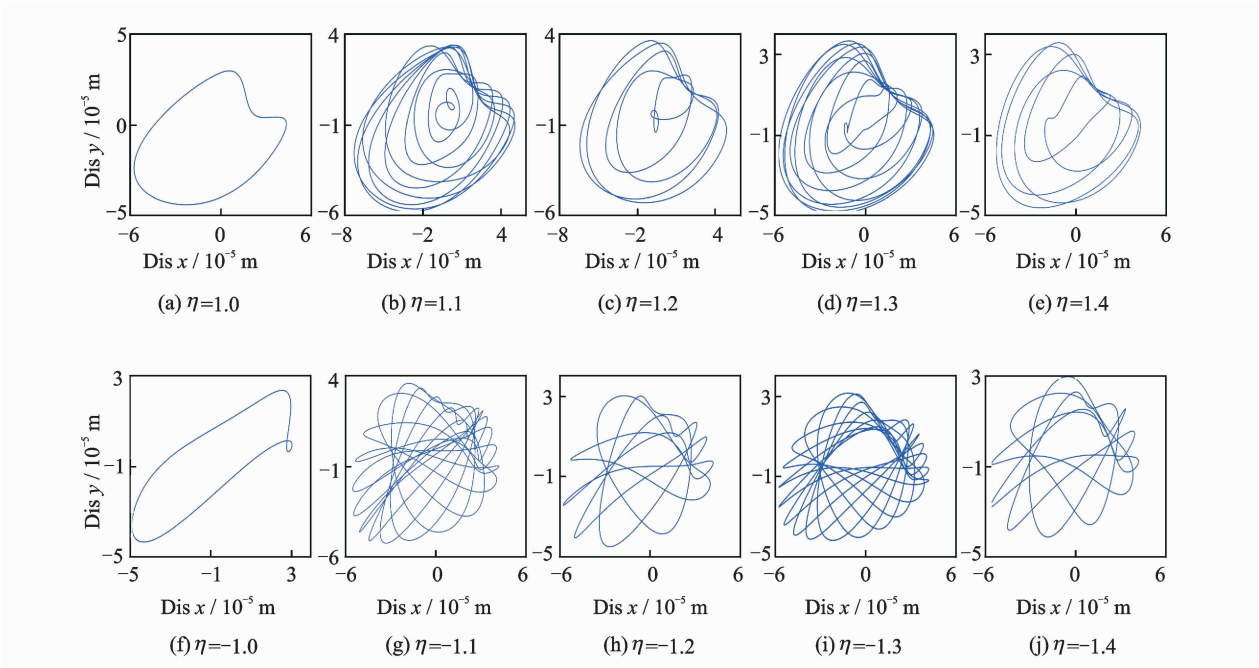

Fig. 8 Motion trajectories of disk 1 under different speed ratios

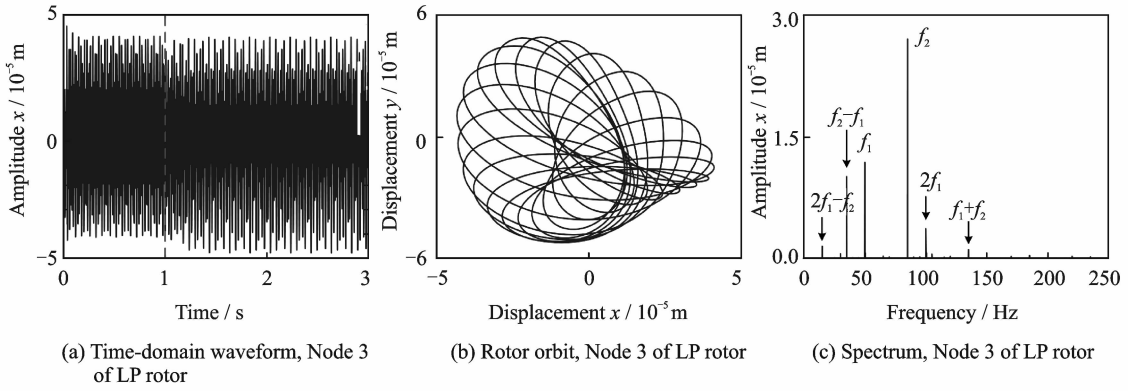

(a) Time-domain waveform, Node 3 of LP rotor (b) Rotor orbit, Node 3 of LP rotor (c) Spectrum, Node 3 of LP rotor

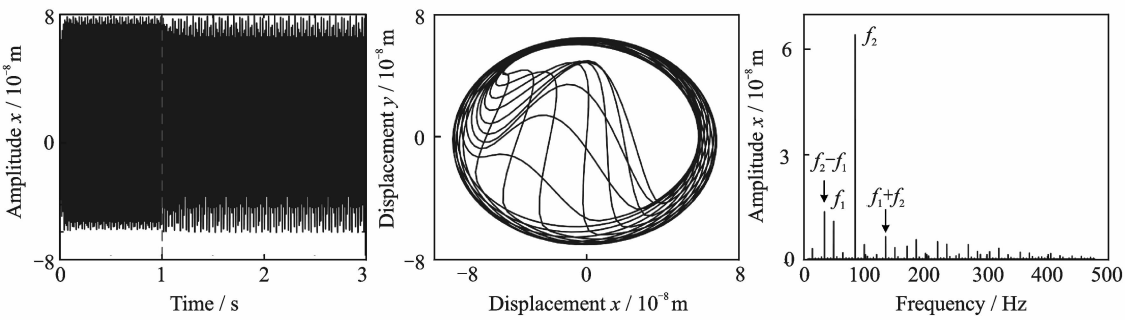

Fig. 9 Rubbing-induced responses with $\eta=-1.7$

Table 2 Simulation parameters

Invariant parameter	Value
Rotational speed Ω/(rev · min^{-1})	3 000
Rubbing stiffness/(N · m^{-1})	$k_r=8\times10^6$
Friction coefficient	$\mu=0.3$
Initial minimum gap/m	$c=1\times10^{-4}$
Unbalance/(kg · m)	$f_{u1}=f_{u2}=f_{u3}=f_{u4}=156\times10^{-6}$
Eccentricity/m	$e=8\times10^{-5}$
Speed ratio	$\eta=-1.7$

3 Conclusions

A FE model of the dual-rotor system with casing is established. Based on shaft center orbits, time-domain waveform, and frequency spectrum, the local rubbing induced nonlinear characteristics of dual-rotor-casing bearing system were analyzed. Some conclusions are summarized as follows:

(1) Besides two unbalanced excitation frequencies and their multiple frequency components, different combined frequency components appear in the spectrum.

(2) The amplitude of torsional vibration under rubbing conditions is larger than that of lateral vibration.

(3) The speed ratio has a great impact on the periodicity of the dual-rotor system. The rubbing-induced response amplitudes under counter-rotation are less than that under co-rotation with the same parameters.

Acknowledgements

This work was supported by the National Natural Science Foundation of China (No. 11772089), the Fundamental Research Funds for the Central Universities (Nos. N160312001 and N160313004), and the Research Project of State Key Laboratory of Mechanical System and Vibration (No. MSV201707).

References:

[1] MUSZYNSKA A. Rotor-to-stationary element subrelated vibration phenomena in rotating machinery: Literature survey [J]. The Shock and Vibration Digest, 1989,21(3):3-11.

[2] HAN Q, ZHANG Z, WEN B. Periodic motions of a dual-disc rotor system with rub-impact at fixed limiter [J]. Proceedings of the Institution of Mechanical Engineers, Part C: Journal of Mechanical Engineering Science, 2008,222(10):1935-1946.

[3] MA H, SHI C, HAN Q, et al. Fixed-point rubbing fault characteristic analysis of a rotor system based on contact theory [J]. Mechanical Systems and Signal Processing, 2013, 38(1):137-153.

[4] TAI X, MA H, LIU F, et al. Stability and steady-state response analysis of a single rub-impact rotor system [J]. Archive of Applied Mechanics, 2015, 85(1):133-148.

[5] CHU F, ZHANG Z. Bifurcation and chaos in a rub-

impact Jeffcott rotor system [J]. Journal of Sound and Vibration, 1998, 210(1): 1-18.

[6] PENG Z, CHU F, PETER W. Detection of the rubbing-caused impacts for rotor-stator fault diagnosis using reassigned scalogram [J]. Mechanical Systems and Signal Processing, 2005, 19(2): 391-409.

[7] MA H, ZHAO Q, ZHAO X, et al. Dynamic characteristics analysis of a rotor-stator system under different rubbing forms [J]. Applied Mathematical Modelling, 2015, 39(8):2392-2408.

[8] YAN L, WANG D. Vibration features from rubbing between rotor and casing for a dual-shaft aeroengine [J]. Journal of Aerospace Power, 1998, 13(2): 173-176. (in Chinese)

[9] YANG Y, CAO D, WANG D, et al. Fixed-point rubbing characteristic analysis of a dual-rotor system based on the Lankarani-Nikravesh model [J]. Mechanism and Machine Theory, 2016, 103: 202-221.

[10] YANG Y, CAO D, YU T, et al. Prediction of dynamic characteristics of a dual-rotor system with fixed point rubbing—Theoretical analysis and experimental study [J]. International Journal of Mechanical Sciences, 2016, 115/116: 253-261.

[11] XU H, WANG N, JIANG D, et al. Dynamic characteristics and experimental research of dual-rotor system with rub-impact fault [J]. Shock and Vibration, 2016(3):1-11.

[12] ZHOU H, CHEN G. Dynamic response analysis of dual rotor-ball bearing-stator coupling system for aero-engine [J]. Journal of Aerospace Power, 2009, 24(6): 1284-1291. (in Chinese)

[13] WANG N, JIANG D, Behdinan K. Vibration response analysis of rubbing faults on a dual-rotor bearing system [J]. Archive of Applied Mechanics, 2017, 87(336):1-17.

[14] LUO G, YANG X, WANG F. Research for response characteristics of rub-impact high-dimensional dual-rotor system [J]. Journal of Vibration Engineering, 2015, 28(1):100-107. (in Chinese)

[15] CHEN G. Vibration modeling and analysis for dual-rotor aero-engine [J]. Journal of Vibration Engineering, 2011, 24(6):619-632. (in Chinese)

[16] HAN Q K, LUO H T, WEN B C. Simulations of a dual-rotor system with local rub-impacts based on rigid-flexible multi-body model [J]. Key Engineering Materials, 2009,413/414:677-682.

[17] WANG N, JIANG D, HAN T. Dynamic characteristics of rotor system and rub-impact fault feature research based on casing acceleration [J]. Journal of Vibroengineering, 2016, 18(3):1525-1539.

Mr. **Ma Xinxing** received his B. S. degree from School of Mechanical and Electrical Engineering, Qingdao University in 2016. In September 2016, he became a post-graduate student at the School of Mechanical Engineering and Automation, Northeastern University. His research has focused on rotor dynamics.

Prof. **Ma Hui** received B. S. degree in Liaoning Technical University in 2002 and Ph. D. degree in Northeastern University in 2007, respectively. From 2007 to present, he has been in the School of Mechanical Engineering and Automation, Northeastern University. In 2013 he was awarded the New Century Excellent Researcher Award Program from Ministry of Education of China. From Nov. 2014 to Oct. 2015, he worked as a visiting scholar in the University of Sheffield, England. His research interests include rotor dynamics and fault diagnosis.

Mr. **Zeng Jin** received B. S. and M. A. degrees in School of Mechanical Engineering and Automation, Northeastern University in 2013 and 2016, respectively. In September 2016, he became a doctoral student at Northeastern University. His research is focused on rotor dynamics.

Mr. **Piao Yuhua** received his B. S. degree from School of Mechanical Engineering and Automation, Northeastern University in 2016. In September 2016, he became a post-graduate student at Northeastern University. His research has focused on rotor dynamics.

(Production Editor: Sun Jing)